RESEARCH PAPER

On-site refractometric determination of composition and component concentrations in hydrocarbon mixtures

Vadim Davydov [a,b], Roman Davydov [c,*], Ekaterina Isupova [d], Linda Boudjemila [e], Olga Vezo [f], Daniil Provodin [a], Roman Klimenko [d], Alexander Belyaev [e]

[a] Higher School of Physics and Materials Technology, Peter the Great St. Petersburg Polytechnic University, Saint-Petersburg, 195251, Russia
[b] Department of Photonics, St. Petersburg Electrotechnical University (LETI), Saint-Petersburg, 197022, Russia
[c] Higher School of Cyberphysical Systems & Control, Peter the Great St. Petersburg Polytechnic University, Saint-Petersburg, 195251, Russia
[d] Department of Optical and Quantum Communication Systems, The Bonch-Bruevich Saint-Petersburg State University of Telecommunications, Saint-Petersburg, 193232, Russia
[e] Department of Physics, The Bonch-Bruevich Saint-Petersburg State University of Telecommunications, Saint-Petersburg, 193232, Russia
[f] Centre for Diagnostics of Functional Materials for Medicine, Pharmacology and Nanoelectronics, St. Petersburg State University, St. Petersburg, 199034, Russia

Abstract

We substantiate the need for a new method that can perform measurements in environments with low optical transparency and high viscosity. Based on prior studies and device capabilities, we note that express hydrocarbon monitoring requires instruments with broad capabilities to handle diverse media. We identify challenges that arise when monitoring the condition of fuel and engine oils using refractometric measurements. A new method has been developed to determine the composition of two-component fuel mixtures (component concentrations) in express monitoring. The design of a refractometer operating on total internal reflection is proposed to implement this method. Various cases can arise when monitoring mixtures of fuels, such as fuel with engine oil or two engine oils. We provide measurement algorithms and reference tables to support implementation of the method. The results of studies of a mixture of two gasoline grades and engine oil with gasoline at different temperatures are discussed and support the method's validity. Directions for further development and research are outlined.

Keywords: Hydrocarbons, Mixtures, Condition monitoring, Refractive index, Density, Concentration

1. Introduction

In the modern world, considerable attention is paid to monitoring the condition of hydrocarbon media (fluids) used across diverse areas of human activity.[1–3] A major application in the field of hydrocarbons is fuel-quality monitoring for vehicles.[1,4–6] This area also includes monitoring the condition of engine oils and lubricants for machinery.[7] There are many reasons for increased condition monitoring of the above-mentioned hydrocarbon liquids. These drivers are mainly determined by two factors: (i) the platform that uses the fuel and (ii) the mission or operating task.[8] Fuels considered include gasoline, aviation kerosene,

Received 22 December 2025; revised 24 February 2026; accepted 25 February 2026.
Available online 6 May 2026

* Corresponding author.
E-mail addresses: davydov_vadim66@mail.ru (V. Davydov), davydovroman@outlook.com (R. Davydov), isupova.e24@mail.ru (E. Isupova), lariessai21@gmail.com (L. Boudjemila), o.vezo@spbu.ru (O. Vezo), provodindanya@gmail.com (D. Provodin), 89213866205@yandex.ru (R. Klimenko), adbelyaev05@gmail.com (A. Belyaev).

https://doi.org/10.62593/2090-2468.1115

diesel fuel, and biofuels. Accordingly, key motivations are[9,10]:

1. Ensuring safe operation, especially for aircraft.
2. Estimating maximum range without refueling,[10–12] which is critical for aircraft, seagoing vessels, and long-distance road transport in sparsely populated areas.[13,14]
3. Preserving engine service life.[11,15] Low-quality fuel causes valves to burn out more quickly, and in some cases, pistons as well.[10,11,16] This may necessitate major engine repairs.[16]

Many methods and instruments have been developed worldwide for controlling hydrocarbons and products derived from them.[2,3,10,17–19] Devices available on the market for measuring hydrocarbon parameters vary in size, accuracy, functionality, and operating conditions.[8,9,20–22] Accordingly, monitoring the quality of fuel and its composition at bases, plants, terminals, airports, and other stationary facilities is less constrained – a number of these methods are successfully used for this purpose.[14,15,21–24] This also applies to large research laboratories and vehicle-diagnostics centers.[17,19,22,25] Not all methods can be used for real-time, on-site monitoring of hydrocarbons and their mixtures at the sampling point, especially outside laboratory environments without compromising instrument functionality and measurement accuracy.[17,24,26–28] These difficulties, only to a lesser extent, can be attributed to the use of several methods in desktop measuring devices, during the operation of which it is necessary to ensure simpler operating conditions than for high-resolution laboratory instruments.[3,9,19,20,29,30] All this, as well as several other factors, led to the fact that the preference has shifted to several classes of instruments – NMR and X-ray spectrometers and selected optical instruments (including spectrometers).[4,9,13,24,31,32] Separately, among the NMR instruments, it is necessary to note NMR relaxometers, which are used to monitor hydrocarbons both in steady-state and flowing conditions.[2,5,19,33–38]

Problems with fuel quality deterioration arise during transfer between containers – e.g., when fueling an aircraft or at a filling station. The container may contain residues of another fuel (e.g., gasoline or aviation kerosene) from prior transport. Two grades may be mixed in unknown proportions.[4,20,29,35,39,40] Hydrocarbon liquids generally do not react chemically with each other; they form miscible liquid mixtures (solutions).[9,13,23,24,35,38] It should be noted that if you mix gasoline and diesel fuel, you can visually determine the presence of one fuel in the other, since they differ in color. When mixing two gasoline grades, it is impossible to distinguish this mixture by color and smell from one of them (detectable only via density/mass measurement with samples of ≈3–5 L, depending on the mixing ratio). Most portable scales are not designed for such masses. This fuel (e.g., a mixture of two gasoline grades or gasoline with kerosene) can be delivered to a fuel station or a vehicle (airplane, helicopter, seagoing vessel, or car, when refueling on the highway). Mobile octane number meters (various models), which allow measurements in the range 75–99.9 with an error of ±1.5–2.0 units (operating temperature range 263–313 K, the required fuel volume is no more than 100 mL) solve this problem up to a certain ratio between the fuel grades when mixing it. When using aviation kerosene or fuel for racing cars, even a small concentration of another fuel (e.g., 1.5–2.0 % of the total volume) in the base fuel is critical. To detect non-compliance of the fuel with the standard in such cases, a refractometer (including a mobile one) with an error in measuring the refractive index n of the order of 0.0001 or less can be used.[8,39–42]

Using a mobile refractometer[39,43–47] also addresses cases of deliberate mixing lower-octane with higher-octane fuel with subsequent restoration of the octane number of the resulting mixture using additives to increase the octane number of high-quality fuel. The question of estimating the octane number when blending two gasolines has been studied for more than fifty years. Based on the results of various studies, the following formula has been proposed to determine the octane number, A_m, of a mixture[48–50]:

$$A_m = K_1A_1 + K_2A_2 \quad (1)$$

where A_1 and A_2 are the octane numbers, for example of gasoline grades (98 and 92), K_1 and K_2 are the volume or mass concentrations in which they are mixed ($K_1 + K_2 = 1$).

When mixing two gasoline grades AI–98 and AI–92 in a ratio of 0.8 to 0.2, the value $A_m = 96.8$. An octane number meter may not detect this difference (the changes are within its measurement error). It is feasible to restore the octane rating to 98 using octane-boosting additives. If a vehicle is designed for AI–98 or higher, operating on a lower effective octane may increase fuel and oil consumption, accelerate valve/piston wear, and lengthen acceleration times.

An elevated octane number achieved by using additives can be retained in gasoline blends for more than two days; thereafter it slowly decreases

toward the true value. The mobile refractometer allows one to determine, based on the change in n, the deviation of a given mixture of two gasolines from the standard corresponding to AI–98 gasoline.

Several problems arise when monitoring hydrocarbon liquids if they are a mixture (e.g., a mixture of two gasoline grades or gasoline–kerosene). In industrial mobile refractometers, n measurements are taken at temperature $T = 293$ K.[8,40,43–47,51,52] In the case of express outdoor fuel monitoring, the device requires time t_s for the appropriate temperature to be established for the medium under study. During time t_s, in the mixture under study, consisting of different types of fuel (especially if it is not well mixed before measurements), there may be a movement of components (e.g., gasoline grades or kerosene) placed on the measuring prism of the refractometer. The heavy fraction will sink to the measuring prism face where the probing beam is incident, and the light fraction will be located on top of the heavier fraction (the lighter fraction will almost not interact with the radiation used for measurements). Table 1 presents the values of density ρ of the main types of fuel used for vehicles and various devices (diesel generators, handheld tools with gasoline engines, burners, camping stoves). The measurements of ρ were made for $T = 288$ K. The range of density values given in parentheses takes into account different concentrations of aromatic hydrocarbons in the fuel.

If the component stratification occurs before the measurement of the refractive index, e.g., a mixture of AI–98 and AI–92 gasoline grades, then reliable determination of the mixture's condition becomes difficult. We consider the main issues below. In the mixture presented in the example, at the prism face the denser component (AI–98) contacts the prism, with the lighter (AI–92) above. A refractometer measures the n value for AI–98 gasoline, which may match the standard value. The mixture will be identified as pure AI–98 gasoline, which does not correspond to reality. Express monitoring may be unreliable under such stratification. Therefore, the test sample must be thoroughly mixed before measurement, which is not always feasible during express monitoring.

Table 1. Values of fuel density ρ at temperature T = 288 K.

Fuel type	Average density, kg/L
Liquefied gas	0.530 ± 0.001
A-76 (unleaded)	0.72467 ± 0.00002
AI-80 (unleaded)	0.73034 ± 0.00002
AI-93 (unleaded)	(0.74027-0.74121) ± 0.00002
AI-95 (unleaded)	(0.74893-0.75088) ± 0.00002
Straight-run aviation kerosene	0.75497 ± 0.00002
AI-95 Premium	(0.75408-0.75876) ± 0.00002
AI-92	0.76026 ± 0.00002
AI-96 (unleaded)	(0.76892-0.77154) ± 0.00002
Aviation kerosene TS2	0.77789 ± 0.00002
AI-98 (unleaded)	(0.77832-0.78234) ± 0.00002
Aviation kerosene TS	0.78033 ± 0.00002
Dearomatized kerosene	0.85027 ± 0.00002
Kerosene	0.81023 ± 0.00002
Fuel T1	0.81887 ± 0.00002
Diesel fuel	0.84012 ± 0.00002
Illuminating kerosene	0.84031 ± 0.00002
Biodiesel fuel	0.87022 ± 0.00002

Gasoline grades pose an additional challenge when monitoring their mixtures using a refractometer, especially for a mixture of AI–95 and AI–92 gasolines. The higher the octane number of a fuel usually means the higher its density. An exception here is that the density of AI–92 gasoline is higher than that of AI–95 (Table 1). When studying this mixture (in the case of a large value of time t_s), the layer of AI–92 gasoline will be located on the edge of the prism used for measurements, and the layer of AI–95 will be located on the layer of AI–92 (from above). Using a refractometer, the value of n will be measured, corresponding to pure AI–92 gasoline (even if its volume concentration in the mixture is 2–3%). In this case, the result of the device's measurement of the octane number will show that the mixture is pure AI–95 gasoline. This apparent contradiction arises because the refractometer probes only the interface in contact with the prism, whereas the octane meter reports a bulk-averaged value.

In other cases, AI–95 gasoline may be sold as AI–92 gasoline (the company will suffer losses). An ordinary fuel buyer, after checking its quality with a refractometer, may file a claim. The measurements showed that fuel of lower quality (AI–92 gasoline) was mistakenly poured into his car's tank. The consumer ordered AI–95 gasoline. Time will be spent on investigating and determining the truth, which is also money and a person's nerves, which are difficult to restore.

Another situation may arise when testing this mixture (AI–95 and AI–92 gasolines) if it is not mixed well. The mixture that forms when mixing two hydrocarbons can be heterogeneous.[35,40,45,53–57] A film with a heterogeneous structure (with spots from the two gasolines AI–92 and AI–95) may form on the edge of the prism where the mixture being tested will be placed. The refractive index n of the medium being tested is determined based on the interaction of radiation with this film using the phenomenon of total internal reflection (TIR).[40,41,44,47,55–58] At the stage of measurement from the structures of two gasolines on the edge of

the prism at the wavelength of visible radiation $\lambda = 589.3$ nm several clear light-shadow boundaries can be formed. It is extremely difficult to obtain reliable measurements in this case. In the worst case, one very wide fuzzy light-shadow boundary is formed. This will lead to a large error when measuring the refractive index n. The reliability of measurements will be low.

Another challenge is unambiguously determining component identities and concentrations from a single n measurement. The measured value of the refractive index in industrial designs of refractometers from the mixture is insufficient to do so. It is necessary to determine the composition and concentration of the components in the mixture so that in the future it would be possible to make an informed decision on using this mixture as a standard fuel (deciding whether an AI–95/AI–92 mixture is acceptable as AI–95). Operational experience (e.g., vehicles, motorboats, diesel generators) suggests that some mixtures may be usable without evident engine issues under certain conditions. In addition, the safety of operating the vehicle and other devices is not violated.

All of this indicates the need for a new real-time method for assessing hydrocarbon media and their mixtures – one that resolves the above issues for fuels and enables unambiguous determination of their composition and component concentrations.

1.1. New method for measuring composition and component concentrations in hydrocarbon mixtures

The following should be considered during the development of the new method: the samplers (dispensers) used for on-site control typically accumulate 5–15 mL of the test medium in a replaceable tip. Our experiments show that 10 mL of the test liquid (e.g., a mixture of AI–92 and AI–95 at 1:99) is sufficient to form an AI–92 layer on the prism face, allowing its refractive index to be measured. Determining the composition of gasoline (or other fuel) mixtures is generally not practically useful when the minor component is below about 1 % (≈1:99), unless deliberate adulteration is suspected.

Consider, for example, the case in which 1 L of AI–80 is accidentally added to 120 L of AI–95. Using equation (1), the octane number of the mixture is $(120 \times 95 + 1 \times 80)/121 = 94.88$, which an octane-rating meter may not detect.

An unpleasant possibility in such a situation is the following: at some moment, the engine cylinder may receive a portion of fuel in which the share of AI–80 is high (e.g., 20 %) with 80 % AI–95. The octane number of such a mixture would then be 92. If the engine is not designed for this octane rating, burn-through may occur and the piston will perform poorly. Over a long operating cycle, however, this would be a similar case (the valves will not burn out). On the other hand, our calculations show that the probability of such an event is less than 0.02 %. For an aircraft, such deterioration in the properties of aviation kerosene is highly undesirable even at this probability during use: during a maneuver, the resulting engine disturbance could cause problems. Therefore, in developing the new method, this must be considered to expand its functional capabilities using the results of measuring n.

The method must also consider sampling constraints: at the point of express fuel monitoring, the use of a dispenser may be volume-limited – or a dispenser may be unavailable. We therefore propose using a plastic sample container with a lid (Fig. 1).

To ensure reliable measurements, the container volume should be at least 10 mL. Such containers are easy to store and transport in a vehicle or bag. Using this container permits vigorous mixing of the test mixture (by shaking). The mixture is then placed on the illuminated prism face of the refractometer and covered with an airtight cap to minimize evaporation. In our laboratory refractometer design, the test mixture is covered by a second prism. We perform measurements at the ambient temperature T_m, after allowing the sample and prism to reach thermal equilibrium; under these conditions the temporal drift is typically 0.1–0.2 K.

Based on experience with various refractometer designs and on studies of liquids performed outside stationary laboratories,[41–43,47,52,54,58] we conclude that an opto-mechanical refractometer is preferable for express monitoring at T_m. This design can measure n using daylight as the illumination

Fig. 1. Sample containers used for on-site fuel collection.

source. Measurements are made at the yellow line of the spectrum, λ = 589.3 nm.

Before loading the prism, the mass of a 10 mL sample is measured. Modern portable electronic scales provide an uncertainty of ±0.02 g. The temperature T_m is also recorded. After placing the mixture on the measuring prism face, the first measurement of its refractive index, n_m, is taken. Two scenarios are common:

(i) The gasoline grade is declared (e.g., AI–95) but contamination by another grade is possible;
(ii) Smell and color indicate gasoline, but the grade is unknown and, if a mixture, so is the composition. The same logic applies to other fuels.

After measurement, n_m is compared with reference $n(T)$ values for fuels at the corresponding temperature T_m. This introduces a practical requirement: users need access to a reference table. Preparing such a table is the instrument manufacturer's responsibility to enable routine use of the method. As an example, Table 2 provides one fragment of such data for AI–92 gasoline. If the measured refractive index n_m matches the standard value n within the measurement uncertainty, express monitoring can be concluded.

Another situation may occur. The value n_m agrees, within the measurement uncertainty, with a refractive-index value for the declared gasoline grade, and glare (specular highlights) is observed in the optical image near the light–shadow boundary. This may indicate that the gasoline contains a small amount of different grade. In this case, wait 3–4 min and perform a second measurement. During this time, the mixture should re-equilibrate and the glare should disappear. The lighter component will rise above the denser one. This indicates the presence of a lower-grade gasoline than the declared grade. This demonstrates that an optical system with visual readout for measuring n has advantages over a fully automatic electronic system.

Subsequently, depending on the intended use of the fuel, it is either approved or sent for additional testing to confirm suitability. For motor vehicles, no operational issues are expected when using such fuel. For aviation – especially long-range flights – the fuel should be examined with high-resolution instruments in a laboratory. After verification, a decision is made on further use.

If, after the sample has been on the prism face for 3–4 min, the glare persists, this indicates the presence of a small amount of a higher-grade gasoline than the declared grade (its fraction remains at the measurement interface where the probing radiation is incident). In this case, no issues are expected with using the declared gasoline grade.

Let us consider the case when the value n_{m} does not correspond to any of the n values associated with standard fuel. We proceed as follows:

1. Repeat the measurement: After the first reading, wait 4–5 min, then measure the refractive index again.
2. Evaluate the second reading: Three outcomes are possible:
   A. Change observed. The new value (denoted n_l^2, i.e., the second-stage reading) matches the declared gasoline grade being tested. Stop measuring. Using the equations developed for the new method determine the mixture composition and component concentrations.
   B. Change observed, but mismatch. The new value n_l^2 does not match the declared grade (e.g., the sample is a two-gasoline mixture such as AI-95 and AI-92). The lower layer is AI-92, and n_l^2 equals its standard refractive index; the sample, however, was declared as AI-95. Stop measuring. Use the developed

Table 2. Temperature dependence of the refractive index n of AI–92 gasoline.

T, K	n (λ = 436.4 nm)	n (λ = 589.3 nm)	n (λ = 657.2 nm)
275.1 ± 0.1	1.4378 ± 0.0001	1.4258 ± 0.0001	1.4231 ± 0.0001
279.2 ± 0.1	1.4358 ± 0.0001	1.4237 ± 0.0001	1.4210 ± 0.0001
283.0 ± 0.1	1.4339 ± 0.0001	1.4216 ± 0.0001	1.4189 ± 0.0001
287.2 ± 0.1	1.4317 ± 0.0001	1.4195 ± 0.0001	1.4168 ± 0.0001
291.0 ± 0.1	1.4296 ± 0.0001	1.4174 ± 0.0001	1.4147 ± 0.0001
293.1 ± 0.1	1.4282 ± 0.0001	1.4161 ± 0.0001	1.4134 ± 0.0001
295.2 ± 0.1	1.4275 ± 0.0001	1.4154 ± 0.0001	1.4127 ± 0.0001
299.0 ± 0.1	1.4253 ± 0.0001	1.4132 ± 0.0001	1.4105 ± 0.0001
303.1 ± 0.1	1.4231 ± 0.0001	1.4111 ± 0.0001	1.4084 ± 0.0001
307.0 ± 0.1	1.4210 ± 0.0001	1.4091 ± 0.0001	1.4065 ± 0.0001
311.2 ± 0.1	1.4191 ± 0.0001	1.4072 ± 0.0001	1.4046 ± 0.0001
315.0 ± 0.1	1.4174 ± 0.0001	1.4057 ± 0.0001	1.4030 ± 0.0001
319.1 ± 0.1	1.4158 ± 0.0001	1.4042 ± 0.0001	1.4014 ± 0.0001

relations to compute the mixture composition and component concentrations.

C. No meaningful change. Within measurement uncertainty, n_m is unchanged; no glare line appears or shifts, and the optical image shows no changes. Classify the gasoline as non-compliant and send a sample to a fixed (stationary) laboratory for chemical or spectral analysis.

In practice, two-component hydrocarbon mixtures dominate – especially with fuels and engine oils. Three-component fuel mixtures occur mainly during tanker transport when handling rules are violated. Intentional blending of three grades or octane boosting with additives is not practiced. In 15 years of hydrocarbon-control work, such mixtures were encountered only twice. Accurately determining their composition requires separate treatment: both specialized data-processing methods for refractive-index measurements and appropriate refractometer designs.

For engine oils, three-component mixtures are more common, typically due to human error (e.g., oil diluted with gasoline, followed by accidental addition of a different oil grade). After the first reading of n_m, users often recognize the mistake and either adjust the blend or discontinue use. Because real-world problems with three-component mixtures are rare, this article does not address them further. For two-component mixtures of engine oils, or oil–gasoline mixtures, the approach to identifying composition and component concentrations is the same as for two-fuel mixtures (gasolines, kerosenes, etc.). In the proposed control method for determining the composition of a mixture consisting of two non-reacting components, it is suggested to use the refraction equation proposed by Ernst Karl Abbe[59,60]:

$$n_m = n_1 K_1 + n_2 K_2 \tag{2}$$

where n_1 and n_2 are the refractive indices of the hydrocarbons that make up the mixture, and K_1 and K_2 are coefficients in relative units corresponding to the concentrations of these components in the mixture, $K_1 + K_2 = 1$.

In (2), the value n_m is determined in the first measurement. The value $n_1 = n_{l_2}$ corresponds to the refractive index measured at the prism surface for the lower layer of the mixture during the second measurement. The value n_2 must be determined, as well as K_1 and K_2. This corresponds to case 1.

For case 2, the two gasoline grades forming the mixture under study are known. In that situation, the values K_1 and K_2 are uniquely determined by solving a system of two linear equations with two unknowns:

$$\begin{cases} n_m = n_{l_2} K_1 + n_2 K_2 \\ K_1 + K_2 = 1 \end{cases} \tag{3}$$

For case 1, the situation is more complex. In system (3), the known quantities are n_m and $n_l{}^2$. The system still contains three unknowns, which creates a problem for obtaining an unambiguous answer for K_1, K_2, and n_2. Therefore, the new method proposes using, together with (3), an additional mass equation:

$$M_m = V_m (\rho_1 K_1 + \rho_2 K_2) \tag{4}$$

where M_m is the mass of the mixture placed in a volume of 10 mL; ρ_1 is the density of the gasoline corresponding to n_l^2; and ρ_2 is the density of the gasoline corresponding to n_2 (the unknown gasoline).

Analysis of the fuel density data (Table 1) makes it possible to identify the gasoline grades that could be located above the gasoline contacting the prism face. This yields several candidate gasoline grades. Next, we consider the following system of equations:

$$\begin{cases} n_m = n_{l_2} K_1 + n_2 K_2 \\ K_1 + K_2 = 1 \\ M_m = V_m (\rho_1 K_1 + \rho_2 K_2) \end{cases} \tag{5}$$

In system (5) there are three unknowns (K_1, K_2, and n_2). The density of a gasoline corresponds uniquely to its refractive index. Given that the number of possible gasoline grades that could lie above the gasoline at the prism face will not exceed three, using (5) allows, by considering these up to three cases, an unambiguous solution for the mixture composition and the concentration values K_1 and K_2.

Similar reasoning applies when the mixture consists of two fuels and the specific grade of the gasoline(s), kerosene(s), etc. under control is not declared. It is assumed only two hydrocarbon components are present in the mixture. In this case, n_m is measured; after some time, the refractive index n_1 at the prism face is measured, which identifies one of the mixture components. Then system (5) and the associated reasoning are used. The values K_1, K_2, and n_2 are determined. From the value of n_2, the second component in the mixture is identified.

1.2. Experimental results

Studies of various hydrocarbon mixtures were conducted using a modified laboratory

refractometer based on TIR. Fig. 2 shows the instrument schematic and the optical ray paths.

In the refractometer, the test mixture is placed between two prisms with gaskets that seal the sample chamber. Fuels (gasolines, kerosenes, etc.) are volatile hydrocarbons; therefore, not every TIR refractometer design is suitable for such studies. In the design shown in Fig. 2, light can reach the prism–sample interface in two ways: through the top cover plate (Fig. 2a) or through the bottom cover plate that carries reflective coating 6 (Fig. 2b). The refractive index of the test medium in contact with the prism is determined from Snell's law and the position of the light–shadow boundary:

$$n_p \sin \alpha_{crit} = n_m \sin \alpha_2 \quad (6)$$

where n_p is the prism refractive index, n_m is the refractive index of the test medium, α_{crit} is the incidence angle at which total internal reflection occurs (the light–shadow boundary forms), and α_2 is the refracted angle (at the critical condition $\alpha_2 = 90°$, so $\sin \alpha_2 = 1$).

In our instrument, n_m is measured as follows. Rotating plate 10 (on which the light–shadow boundary is registered) changes the angle of incidence by the optical design (Fig. 2). The n_m scale is calibrated using (6) so that, when the boundary is aligned with the plate crosshair, (6) holds with $\sin \alpha_2 = 1$, and n_m is read from the critical angle. The lower scale visible beneath the boundary in the eyepiece is illustrated in Figs. 3–5 for measurements of neat gasolines and their mixtures.

As an example, demonstrating the new method's ability to determine mixture composition and component concentrations, we present results for a gasoline mixture of AI–92 and AI–80 in a 7:3 ratio (10 mL sample). Such mixtures commonly arise from improper storage (container changes) or

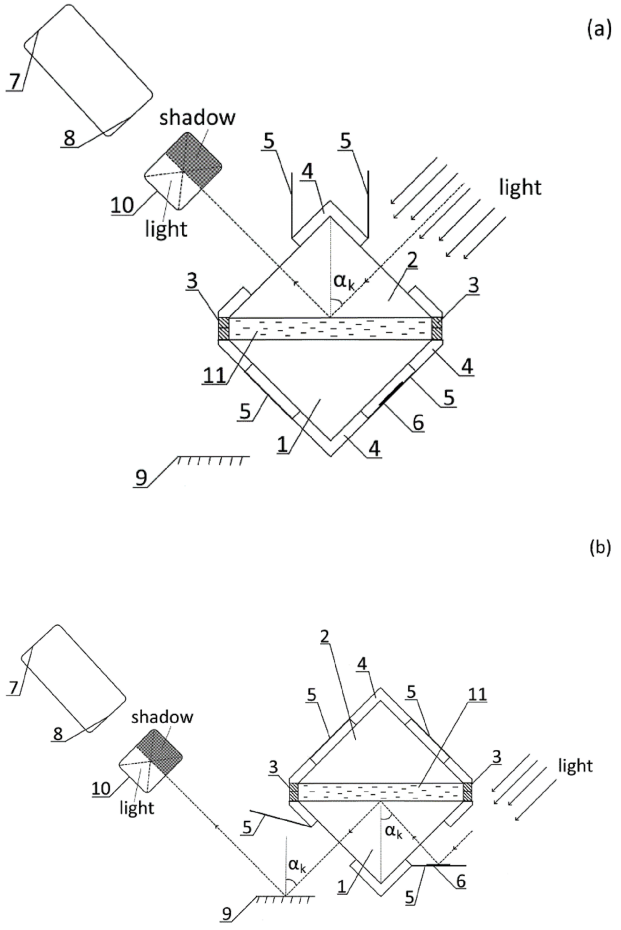

Fig. 2. a. Schematic for refractive-index measurement at the interface between the upper prism face and the test hydrocarbon: 1 – lower prism, on whose upper face the test medium is placed; 2 – upper prism covering the test medium; its base contacts the medium; 3 – gaskets forming a sample chamber; when the upper prism is lowered, the chamber is sealed; 4 – prism-rotation couplings; 5 – movable opaque shutters; 6 – reflective coating; 7 – eyepiece; 8 – objective lens; 9 – tilting (pivoting) mirror; 10 – reticle (crosshair) plate used to register the light–shadow (critical-angle) boundary; 11 – test hydrocarbon or a mixture thereof. b. Schematic for refractive-index measurement at the interface between the lower prism face and the test hydrocarbon: 1 – lower prism, on whose upper face the test medium is placed; 2 – upper prism covering the test medium; its base contacts the medium; 3 – gaskets forming a sample chamber; when the upper prism is lowered, the chamber is sealed; 4 – prism-rotation couplings; 5 – movable opaque shutters; 6 – reflective coating; 7 – eyepiece; 8 – objective lens; 9 – tilting (pivoting) mirror; 10 – reticle (crosshair) plate used to register the light–shadow (critical-angle) boundary; 11 – test hydrocarbon or a mixture thereof.

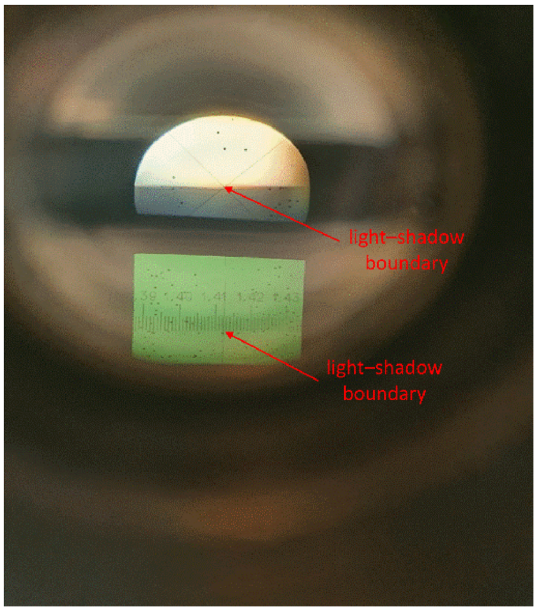

Fig. 3. Eyepiece view of the light–shadow boundary and the measurement result for the gasoline mixture (first measurement).

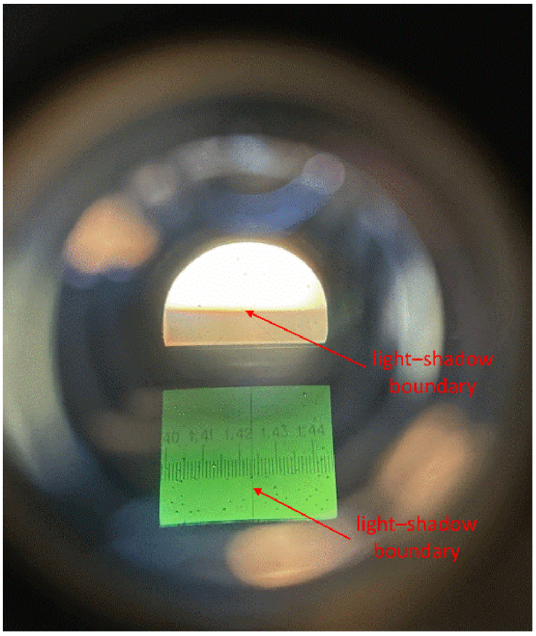

Fig. 4. Eyepiece view of the light–shadow boundary and the measurement result for the gasoline mixture (second measurement).

tanker transport. We consider the case in which the mixture has not been declared as a specific gasoline grade and the composition and usability must be established. Figs. 3–5 show the eyepiece view of the n_m scale and the light–shadow boundary at the crosshair.

Following the developed method, a 10 mL portion of the mixture in the container (Fig. 1) was shaken and placed on the upper face of the lower prism (part 1) of the refractometer (Fig. 2). It was then covered with the upper prism (part 2). The initial reading was $n_m = 1.4121 \pm 0.0002$ at $T = 300.3$ K (Fig. 3). The obtained value does not correspond to any refractive-index value of standard fuels. After waiting 260 s, the second reading was $n_1 = 1.4235 \pm 0.0002$ at the same temperature (Fig. 4), which corresponds to AI–92 gasoline. For verification, a control measurement of AI–80 gasoline was also taken, yielding $n_2 = 1.385 \pm 0.0002$ at T = 300.3 K (Fig. 5).

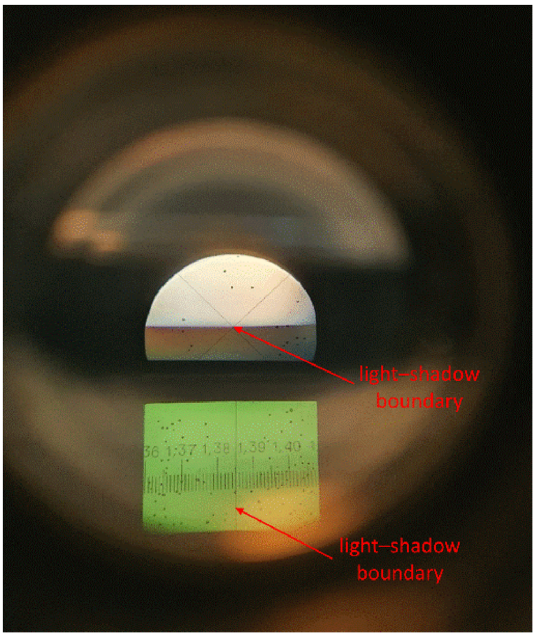

Fig. 5. Eyepiece view of the light–shadow boundary and the measurement result for AI–80 gasoline (control measurement).

Based on our method and the density data in Table 1, the possible second component in the mixture could be one of the following: A–76 (unleaded), AI–80 (unleaded), AI–93 (unleaded), AI–95 (unleaded), straight-run aviation kerosene, or AI–95 Premium. In principle, using equation (5), all candidate second components can be evaluated and the actual component present can be identified unambiguously. As a practical strategy, begin with grades whose octane number is lower than AI–92, the grade identified in the mixture. If higher-octane grades such as AI–93 (unleaded), AI–95 (unleaded), or AI–95 Premium are added to AI–92, the resulting fuel is generally acceptable for engine operation. Straight-run aviation kerosene is unlikely to be present in AI–92 gasoline.

Express monitoring is performed over a wide temperature range. Therefore, density values must be available for that range. Numerous studies have addressed this need,[17,19,20,51,61] enabling the following empirical relation for gasoline density as a function of temperature:

$$\rho(T) = \rho_b + \Delta\rho\Delta T \tag{7}$$

where ρ_b is the density at $T = 293.0 \pm 0.1$ K, $\Delta\rho$ is the temperature coefficient of density (see Table 3), and ΔT is the deviation of the measurement temperature T_m from 293.0 ± 0.1 K ($293 - T_m$).

To apply equation (7), the $\Delta\rho$ value is used together with the density data from Table 3. Table 3 was compiled by representatives of Russian oil companies and producers of various hydrocarbons. Similar tables are used in other countries.

As an example, Fig. 6 shows the temperature dependence of density ρ for AI–80 and AI–92 gasolines used to prepare the test mixture.

To validate our method, we used equation (5) and relation (7) with the data in Table 3 and evaluated all previously listed gasoline candidates that could serve as the second component in the mixture (straight-run aviation kerosene was excluded; in

Table 3. Temperature corrections to the density of petroleum products relative to $T = 293.0 \pm 0.1K$.

Density (ρ, g/cm^3)	Temperature correction per 1K (Δρ, g/cm^3)	Density (ρ, g/cm^3)	Temperature correction per 1K (Δρ, g/cm^3)
(0.6500–0.6598) ± 0.0001	0.000962	(0.8300–0.8398) ± 0.0001	0.000725
(0.6600–0.6698) ± 0.0001	0.000949	(0.8400–0.8498) ± 0.0001	0.000712
(0.6700–0.6798) ± 0.0001	0.000936	(0.8500–0.8598) ± 0.0001	0.000699
(0.6800–0.6898) ± 0.0001	0.000925	(0.8600–0.8698) ± 0.0001	0.000686
(0.6900–0.6998) ± 0.0001	0.000910	(0.8700–0.8798) ± 0.0001	0.000673
(0.7000–0.7098) ± 0.0001	0.000897	(0.8800–0.8898) ± 0.0001	0.000660
(0.7100–0.7198) ± 0.0001	0.000884	(0.8900–0.8998) ± 0.0001	0.000647
(0.7200–0.7298) ± 0.0001	0.000870	(0.9000–0.9098) ± 0.0001	0.000633
(0.7300–0.7398) ± 0.0001	0.000857	(0.9100–0.9198) ± 0.0001	0.000620
(0.7400–0.7498) ± 0.0001	0.000844	(0.9200–0.9298) ± 0.0001	0.000607
(0.7500–0.7598) ± 0.0001	0.000831	(0.9300–0.9398) ± 0.0001	0.000594
(0.7600–0.7698) ± 0.0001	0.000818	(0.9400–0.9498) ± 0.0001	0.000581
(0.7700–0.7798) ± 0.0001	0.000805	(0.9500–0.9598) ± 0.0001	0.000567
(0.7800–0.7898) ± 0.0001	0.000792	(0.9600–0.9698) ± 0.0001	0.000554
(0.7900–0.7998) ± 0.0001	0.000778	(0.9700–0.9798) ± 0.0001	0.000541
(0.8000–0.8098) ± 0.0001	0.000765	(0.9800–0.9898) ± 0.0001	0.000528
(0.8100–0.8198) ± 0.0001	0.000752	(0.9900–0.9998) ± 0.0001	0.000515
(0.8200–0.8298) ± 0.0001	0.000738		

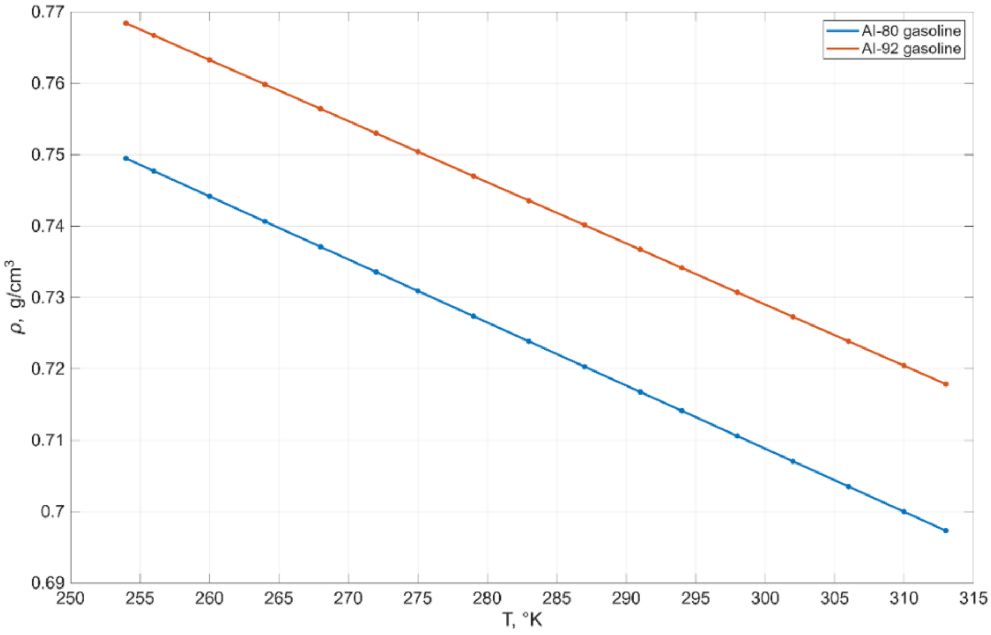

Fig. 6. Temperature dependence of density ρ for AI–80 and AI–92 gasolines.

applications where it is used, AI–95 or higher is specified rather than AI–92). This yielded $n_2 = 1.385 \pm 0.002$ (at $T = 300.3$ K), $K_1 = 0.7021 \pm 0.0015$, and $K_2 = 0.2979 \pm 0.0015$. The value n_2 corresponds to AI–80 gasoline and differs from the control measurement in Fig. 5 by less than the refractometer's measurement uncertainty (0.0002). The coefficients K_1 and K_2 agree, within measurement uncertainty, with the intended composition of the prepared mixture (AI–92 and AI-80).

Additionally, we examined how the refractive index of a Group III, SAE 5W-30 engine oil changes over a small temperature range in two states. The results are shown in Fig. 7. The observed trends agree with earlier studies on various oils.[37,55,62,63]

1.3. Measurement uncertainties of the new method

Modern instruments provide high-precision measurements under laboratory conditions. To measure the density of fuel and other

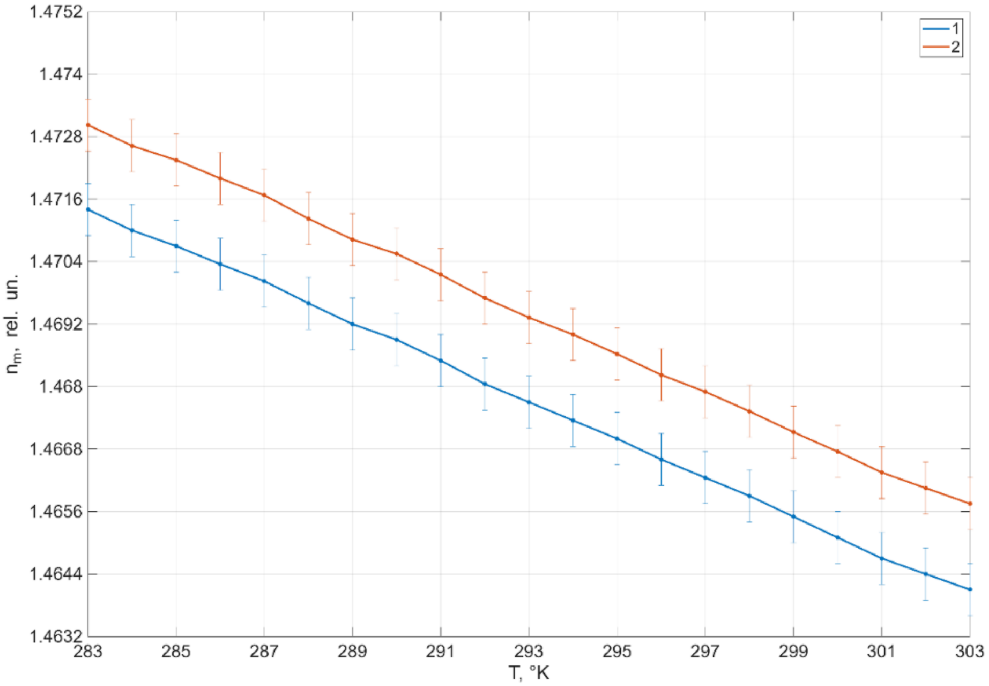

Fig. 7. Temperature dependence of the refractive index n_m of engine oil. Curves: 1 – oil containing AI–80 gasoline (oil:gasoline = 9:1); 2 – neat oil.

hydrocarbons, we used a DSA 5000 M density meter with an uncertainty of 0.00002 g/mL. When using a mobile density meter, density measurements can be performed with an uncertainty of 0.0001 g/mL (we used this value in Table 3).

An analysis of fuel-density data for fuels with different aromatic-hydrocarbon contents allows us to conclude that the relative uncertainty of the density measurement ρ, which is on the order of 0.01%, does not have a significant effect on the uncertainty in determining K_1 and K_2 using relationships (5).

The temperature of the medium under study is controlled with an uncertainty of ±0.1 K (a standard value for measuring instruments). When the temperature T changes by 0.1 K, the refractive index of the liquid medium changes in the fifth decimal place, which is not relevant for express monitoring. These changes in n can be monitored only with a stationary laboratory refractometer.

The density of the liquid medium, as shown by our measurements using the DSA 5000 M density meter, changes (when T changes by 0.1 K) in the fifth decimal place as well. Therefore, the uncertainty in measuring T does not affect the uncertainty in determining the coefficients K_1 and K_2.

To determine the uncertainty with which the coefficients K_1 and K_2 are established, let us consider two equations from relationships (5):

$$K_1 + K_2 = 1 \tag{8}$$

$$M_m = V_m\,(\rho_1 K_1 + \rho_2 K_2) \tag{9}$$

In the method, the mass M_m of a 10 mL container is measured using portable scales (mass-measurement uncertainty is ±0.02 g). The relative uncertainty of mass measurement, provided that an object with a mass greater than 10 g is being measured, is less than 0.2%.

When filling the control volume using a dispenser, the uncertainty of volume formation (measurement) is ±0.05 mL (0.5%). In accordance with relationship (9), the main contribution to the uncertainty in determining K_1 and K_2 will come from the uncertainty of the ratio M_m/V_m.

The values K_1 and K_2 are determined in relative units with respect to the value 1. Therefore, to estimate the uncertainty, one can use the formula for the uncertainty of a quotient:

$$\delta\left(\frac{a}{b}\right) \le \frac{\delta(a)+\delta(b)}{1-\delta(b)} \tag{10}$$

In the considered example of determining the composition of the medium and the concentration of components, $\delta(a) = \delta(b)$. The uncertainty in determining the coefficients K_1 and K_2 is on the order of 0.7% (third decimal place).

The refractive index n_2 is computed with the same uncertainty, because the uncertainty in determining n_m is almost an order of magnitude smaller. For n_m, the third decimal place is guaranteed. This

information is sufficient to determine the fuel grade and the condition (status) with respect to aromatic hydrocarbons.

The uncertainty in determining K_1 and K_2 can be reduced by using a vessel with a volume of 50 mL for measurements. In this case, according to (10), the uncertainty will be determined by the error in filling it with fuel (there is no 50 mL dispenser). It is difficult to say how much fuel will be lost to evaporation (this depends on experience working with hydrocarbons). The uncertainty of the mass measurement will decrease by almost a factor of five. In the future, the uncertainty of measuring K_1 and K_2 can be reduced to 0.01%. For express monitoring it is enough.

2. Discussion

The example presented for a mixture of two gasolines (AI−92 and AI−80) extends directly to other two-grade mixtures. The sequence of actions and measurements, guided by intermediate results, remains unchanged − this illustrates the broad applicability of the method.

Placing the test mixture on the refractometer's lower prism remains straightforward across mixtures (including gasoline−motor-oil mixtures). Under our procedure, evaporation was minimal during sample loading and did not materially affect refractive-index measurements or the subsequent determination of mixture composition and component concentrations.

The proposed relation (7) for calculating density ρ as a function of temperature T, together with the correction tables, yields $\rho(T)$ values that agree well with our measurements for AI−80 and AI−92 using a density meter with a temperature-controlled bath. For these grades (Fig. 6), calculated and measured $\rho(T)$ agreed within the measurement uncertainty.

For the dependences in Fig. 7 (engine oil and its mixture), the slope of curve 1 increases with temperature. This is consistent with the mixture's composition and thermal-expansion behavior (density change with T). We also applied the composition-determination procedure to this mixture. After a settling period, the engine oil occupies the measurement interface at the prism face, with AI-80 gasoline above it. The inferred fractions were $K_1 = 0.901 \pm 0.007$ and $K_2 = 0.099 \pm 0.007$. The inferred refractive index for AI-80 differed from the refractometer reading by less than the instrument's uncertainty. The errors in determining the coefficients K_1 and K_2 are <0.5%, which fully satisfies the express monitoring requirements across different media. These results further confirm the validity of the developed method.

As part of the discussion of the proposed method, it is worth considering various cases in which the fuels forming the mixture have different concentrations of aromatic hydrocarbons. In the Russian Federation, different aromatic-hydrocarbon concentrations are encountered in gasoline grades AI-95, AI-95 Premium, AI-96, AI-98, and AI-100.

Gasoline grade AI-92 has an aromatic-hydrocarbon concentration that classifies it as having medium aromatic content. When fuel is supplied to a consumer, its grade and the data on its aromatic content are declared. A problem may arise only when it is necessary to perform express monitoring of an unknown fuel that may be a mixture.

From the measured value of the refractive index of one of the hydrocarbons (the one that will be at the lower level), one can determine one of three fuel states: low aromatic content, medium aromatic content, or high aromatic content. As the concentration of aromatic hydrocarbons in the fuel increases, the value of n increases. There is a minimum and maximum percentage of aromatic hydrocarbons for each fuel grade.

For each gasoline grade, changes in refractive index occur in the second decimal place when the aromatic-hydrocarbon content changes (low aromatic content, medium aromatic content, high aromatic content). After determining the fuel grade, following the second refractive-index measurement there is information about the other component of the mixture, whose density must be lower than that of the identified fuel. Next, density values are selected for possible variants of this component, considering the possible aromatic-hydrocarbon concentration for that fuel grade.

For gasoline grades AI-96, AI-98, and AI-100, three fuel-state variants must be considered (low aromatic content, medium aromatic content, high aromatic content). For AI-95 Premium and AI-95, two fuel-state variants must be considered (medium aromatic content and high aromatic content). For AI-92, only the medium aromatic-content state is required. This also applies to gasoline grades AI-93, AI-80, and A-76. For all possible variants, using (5), the coefficients K_1 and K_2 are determined, and then n_2 is computed. Considering the additional cases will increase calculation time by at most 2−3 s, which is not critical for express monitoring. The principle of applying the new method does not change.

It should also be noted that the data on aromatic-hydrocarbon concentrations in different gasoline grades refer to fuel produced within the territory of the Russian Federation. These data may differ from those for fuels produced in other countries.

3. Conclusions

Analysis of studies conducted over a range of temperature (including sub-zero values) using our previously developed laboratory refractometer design, together with the obtained data on the composition of various hydrocarbon mixtures and their component concentrations, confirms the rationale for implementing the new method to achieve unambiguous real-time control of fuels and motor oils at the sampling point.

The same laboratory refractometer design can also be used to:

(i) monitor the state of most liquid media (excluding a few aggressive liquids, chiefly acids such as hydrofluoric acid);
(ii) measure refractive indices of solids; and (iii) assess homogeneity in transparent materials.

Finally, with minor modifications to equation (5), the method can be extended to three-component hydrocarbon mixtures. This requires upgrading the optical readout so that refractive indices from two layers (light and heavy fractions) can be read on a single instrument scale. Field deployment then becomes practical. The first measured layer at the lower prism face corresponds to the densest fraction; the second layer, contacting the upper prism face, corresponds to the lightest fraction. From these two n values the grades of the outer layers (gasolines, kerosenes, or oils) can be identified; the third, intermediate fraction can then be inferred using Table 1. With these inputs, a modified three-equation system (unknowns K_1, K_2, K_3 with $K_1 + K_2 + K_3 = 1$) yields a unique solution. If two candidates are plausible for the intermediate fraction, the system is solved twice; only one solution will be consistent. This underscores the method's functional breadth, which we plan to expand through further studies.

Funding

The study was carried out at the Centre for Diagnostics of Functional Materials for Medicine, Pharmacology and Nanoelectronics of the Research Park of St. Petersburg State University within the framework of project 125021702335-5.

Author contributions

Vadim Davydov: Conceptualization, Formal analysis, Methodology, Project administration, Supervision, Validation, Writing – original draft. Roman Davydov: Conceptualization, Formal analysis, Investigation, Methodology, Validation, Visualization, Writing - review & editing. Ekaterina Isupova: Conceptualization, Investigation, Resources, Visualization. Linda Boudjemila: Investigation, Validation. Daniil Provodin: Formal analysis, Investigation, Software. Roman Klimenko: Formal analysis, Investigation, Software.

Ethics information

This study did not involve human participants or animals. Therefore, ethical approval was not required.

Acknowledgements

The authors acknowledge the Centre for Diagnostics of Functional Materials for Medicine, Pharmacology and Nanoelectronics of the Research Park of St. Petersburg State University for providing access to the research facilities and instrumentation used in this study.

Conflict of interest

The authors declare that they have no known competing financial interests or personal relationships that could have appeared to influence the work reported in this paper.

References

1. Zhang X, Wang H, Li J, et al. Effect of heavy aromatic structures on particulates emission of GDI vehicles under WLTC and RDE conditions. *Fuel*. 2025;401:135712. https://doi.org/10.1016/j.fuel.2025.135712.
2. Kashaev RS, Ovseenko GA, Kozelkova VO, Karachin VI, Kozelkov OV. Technology of application of a hardware and software complex based on the PMR relaxometry method for express monitoring of crude oil characteristics with gas analysis in an explosive zone. *Theor Found Chem Eng*. 2025;59(1):95–99. https://doi.org/10.1134/S0040579525700186.
3. Tajik A, Vakhin AV, Nazimov NA, et al. Investigating the effect of microwave radiation at different frequencies on improving the quality of heavy oil. *Fuel*. 2024;375:132547. https://doi.org/10.1016/j.fuel.2024.132547.
4. Xu C, Gao Y, Liu J, et al. Formation mechanisms of composite continental-margin basins and their control of hydrocarbon accumulation: a case study of the Pearl River Mouth Basin, northern South China Sea. *Oil Gas Geol*. 2025;46(3):719–739. https://doi.org/10.11743/ogg20250303.
5. Kashaev RS, Kozelkova VO, Ovseenko GA, Karachin VI, Kozelkov OV. Multiparametric flow-through measuring complex for express control of oil quality using a proton magnetic resonance relaxometry method. *Meas Tech*. 2023;66(5):349–358. https://doi.org/10.1007/s11018-023-02234-5.
6. Donskaya NO, Goldberg MA, Fomin AS, et al. Novel catalysts based on synthetic mesoporous silicates of the MCM-41 type and hydroxyapatite for desulfurization of model fuel. *Ceramics*. 2025;8(2):61. https://doi.org/10.3390/ceramics8020061.
7. Özdemir E, Kan E, Guo B, et al. The role of polyisobutylene-bis-succinimide (PIBSI) dispersants in lubricant oils on the deposit control mechanism. *Polymers*. 2025;17(8):1041. https://doi.org/10.3390/polym17081041.

8. Korneva I, Sinyavsky N, Kostrikova N. Marine motor oils refractometry. *AIP Conf Proc*. 2024;3243(1):020106. https://doi.org/10.1063/5.0247383.
9. Rudszuck T, Nirschl H, Guthausen G. Combined nuclear magnetic resonance methods in quality control of lubricants in green energy production. *Magn Reson Chem*. 2024;62(4):212–221. https://doi.org/10.1002/mrc.5339.
10. Hogan H. Toyota study: better antioxidants, higher quality base oils could be important in preventing turbocharger coking. *Fuels Lubes Intern*. 2016;22(2):20–23 (no DOI).
11. Xu Z, Fan Y, Zheng Y, et al. Emission reduction characteristics of heavy-fuel aircraft piston engine fueled with 100% HEFA sustainable aviation fuel. *Environ Pollut*. 2025;368:125661. https://doi.org/10.1016/j.envpol.2025.125661.
12. Fuchs C, Arnold U, Sauer J. Synthesis of sustainable aviation fuels via (co-)oligomerization of light olefins. *Fuel*. 2025;382:133680. https://doi.org/10.1016/j.fuel.2024.133680.
13. Xue X, Sung C-J, Wang X. Experimental evaluation of binary iso-dodecane/n-dodecane blends for emulating sooting characteristics of sustainable aviation fuels. *SAE Intern J Aerospace*. 2025;18(1):33–45. https://doi.org/10.4271/01-18-01-0003.
14. Karthika AM, Thomas T, Augustine C, Arun Luiz T, Scaria R. DFT-based computational analysis of 2,4-dimethyl-6-tert-butylphenol (DTBP) as an antioxidant in aviation fuels. *Mol Phys*. 2025;123(10):e2393435. https://doi.org/10.1080/00268976.2024.2393435.
15. Wang Y, Zhou Q. Impacts of injection parameters on the mixture formation and performance of two-stroke spark-ignition direct-injection aviation kerosene engine. *J Energy Resour Technol*. 2024;146(2):022302. https://doi.org/10.1115/1.4063925.
16. Hou L, Wang Y, Zheng Y, Zhang A. The impact of vehicle ownership on carbon emissions in the transportation sector. *Sustainability*. 2022;14(19):12657. https://doi.org/10.3390/su141912657.
17. Zhang S, Zhao Z, Wang L, et al. Experimental study on the effects of injection pressure on the combustion in a SI aviation piston engine fueled with kerosene. *Fuel*. 2023;354:128875. https://doi.org/10.1016/j.fuel.2023.128875.
18. Amhamed AI, Assaf AHA, Le Page LM, Alrebei OF. Alternative sustainable aviation fuel and energy (SAFE) – a review with selected simulation cases of study. *Energy Rep*. 2024;11:3317–3344. https://doi.org/10.1016/j.egyr.2024.03.002.
19. Staš M, Kittel H, Matějovský L, Kejla L, Šimáček P. General methods for the analysis of physical properties of fuels. *Paliva*. 2023;15(3):126–135. https://doi.org/10.35933/paliva.2023.03.07.
20. Wang L, Zhao Z, Yu C, Cui H. Experimental study of aviation kerosene engine with PJI system. *Energy*. 2022;248:123590. https://doi.org/10.1016/j.energy.2022.123590.
21. Wei S, Sun L, Wu L, Yu Z, Zhang Z. Study of combustion characteristics of diesel, kerosene (RP-3) and kerosene-ethanol blends in a compression ignition engine. *Fuel*. 2022;317:123468. https://doi.org/10.1016/j.fuel.2022.123468.
22. Zhao Z, Cui H. Numerical investigation on combustion processes of an aircraft piston engine fueled with aviation kerosene and gasoline. *Energy*. 2022;239:122264. https://doi.org/10.1016/j.energy.2021.12226.
23. Yu L, Wu H, Zhao W, et al. Experimental study on the application of n-butanol and n-butanol/kerosene blends as fuel for spark-ignition aviation piston engine. *Fuel*. 2021;304:121362. https://doi.org/10.1016/j.fuel.2021.121362.
24. Ning L, Duan Q, Wei Y, et al. Experimental investigation on combustion and emissions of a two-stroke DISI engine fueled with aviation kerosene at various compression ratios. *Fuel*. 2020;259:116224. https://doi.org/10.1016/j.fuel.2019.116224.
25. Turlybekova G, Kenbay A, Aldiyarov A, et al. Cryogenic system for FTIR analysis of hydrocarbon fuels at low temperature and atmospheric pressure. *Appl Sci*. 2025;15(14):7944. https://doi.org/10.3390/app15147944.
26. Liu S, Hou S, Liu Z. Comparative study, prospects, and suggestions of air-pollutant control standards related to the petrochemical industry source between China and the United States. *Hua Gong Jin Zhan*. 2024;43(7):4089–4101. https://doi.org/10.16085/j.issn.1000-6613.2023-1874.
27. Tang R, Guo S, Song K, et al. Emission characteristics of intermediate-volatility organic compounds from a Chinese gasoline engine under varied operating conditions: influence of fuel, velocity, torque, rotational speed, and after-treatment device. *Sci Total Environ*. 2024;906:167761. https://doi.org/10.1016/j.scitotenv.2023.167761.
28. Shi G, Yang R, Zhao N, et al. Rapid detection method of total amount of aromatic hydrocarbons in soil based on fluorescence imaging technology. *Guangxue Xuebao*. 2023;43(6):0612005. https://doi.org/10.3788/AOS221436.
29. Othman AR, Zain SM, Low KH. Multivariate calibration strategy in simultaneous determination of temperature properties of petroleum diesel by near-infrared spectrometry. *J Near Infrared Spectrosc*. 2022;30(5):237–245. https://doi.org/10.1177/09670335221130425.
30. Yu H, Wang X, Shen F, Long J, Du W. Novel automatic model construction method for the rapid characterization of petroleum properties from near-infrared spectroscopy. *Fuel*. 2022;316:123101. https://doi.org/10.1016/j.fuel.2021.123101.
31. Xiong T, Meng M, Wang N, et al. Investigation on desorption of petroleum hydrocarbon contaminants by active and passive particle self-rotation. *J Environ Chem Eng*. 2021;9(6):106330. https://doi.org/10.1016/j.jece.2021.106330.
32. Yu H, Du W, Lang Z-Q, Wang K, Long J. A novel integrated approach to characterization of petroleum naphtha properties from near-infrared spectroscopy. *IEEE Trans Instrum Meas*. 2021;70:9423975. https://doi.org/10.1109/TIM.2021.3077659.
33. Kashaev RS, Kien NT, Tung CV, Kozelkov OV. Correlation of physicochemical properties of bach Ho oils with proton NMR relaxation parameters and their temperature dependence. *Petrol Chem*. 2019;59:S21–S29. https://doi.org/10.1134/S0965544119130073.
34. Davydov VV, Moroz AV, Myazin NS, Makeev SS, Dudkin VV. Peculiarities of registration of the nuclear magnetic resonance spectrum of a condensed medium during express control of its state. *Opt Spectrosc*. 2020;128(10):1678–1685. https://doi.org/10.1134/S0030400X20100082.
35. Kashaev RS, Kien NC, Tung TV, Kozelkov OV. Fast proton magnetic resonance relaxometry methods for determining viscosity and concentration of asphaltenes in crude oils. *J Appl Spectrosc*. 2019;86(5):890–895. https://doi.org/10.1007/s10812-019-00911-4.
36. Davydov VV, Dudkin VI, Myazin NS, Davydov RV. On the possibility of studying ferrofluids by a nuclear magnetic magnetometer with a flowing sample. *J Commun Technol Electron*. 2020;65(5):558–564. https://doi.org/10.1134/S1064226920050010.
37. Karabegov MA. The dynamic characteristics of automatic analyzers. *Meas Tech*. 2013;55(11):1301–1310. https://doi.org/10.1007/s11018-013-0125-1.
38. Davydov VV, Myazin NS, Davydov RV. Nuclear-magnetic flowmeter-relaxometer for monitoring the flow rate and state of the coolant in the first loop of the nuclear reactor of a moving object. *Meas Tech*. 2022;65(4):279–289. https://doi.org/10.1007/s11018-022-02080-x.
39. Karabegov MA. Flame photometers: basic parameters and metrological support. *Meas Tech*. 2011;54(6):735–742. https://doi.org/10.1007/s11018-011-9796-7.
40. Karabegov MA. Some metrological problems of analytical measurements. *Meas Tech*. 2009;52(1):97–104. https://doi.org/10.1007/s11018-009-9224-4.
41. Davydov VV, Grebenikova NM, Smirnov KY. An optical method of monitoring the state of flowing media with low transparency that contain large inclusions. *Meas Tech*. 2019;62(6):519–526. https://doi.org/10.1007/s11018-019-01655-5.
42. Hu Q, Zhang J, Wang K, Qian L. Refractive index sensor with finite dimensions based on a topological guided-mode

resonance grating. *Opt Laser Technol*. 2025;192:113487. https://doi.org/10.1016/j.optlastec.2025.113487.
43. Ren Z, Zhu X, Zhang D, et al. A reflective hybrid sensor for dual-parameter measurement of refractive index and temperature. *Opt Commun*. 2025;595:132352. https://doi.org/10.1016/j.optcom.2025.132352.
44. Roshani S, Yahya SI, Karami P, et al. Intelligent photonic crystal-based optical sensor for accurate glycerol–water mixture measurement using artificial neural networks. *Opt Mater Express*. 2025;15(7):1710–1729. https://doi.org/10.1364/OME.562971.
45. Tan X, Chen J, Yan S, Zhang H, Sun C. Dynamic refractive index measurement method for droplets based on digital image correlation and inverse method. *Meas Sci Technol*. 2025;36(6):065015. https://doi.org/10.1088/1361-6501/addf6a.
46. Rososhek A, Kusse BR, Potter WM, et al. Wavenumber calibration for an imaging refractometer. *J Appl Phys*. 2025;137(23):234505. https://doi.org/10.1063/5.0265811.
47. Chen S, Zhang C, Bai X, Zhang M, Su J. Influence of sodium silicate on the refractive index of seawater using a CMOS-module-based refractometer. *Infrared Laser Eng*. 2025;54(5):20250078. https://doi.org/10.3788/IRLA20250078.
48. Li Y, Lin S, Zhou X, Wu G. An improved manifold-projection trajectory based method for chemical kinetic mechanism reduction. *Chem Eng Sci*. 2024;298:120416. https://doi.org/10.1016/j.ces.2024.120416.
49. Feng H, Li X, Wang X, Nan Z. Octane blending effect of ethanol-gasoline in high-strength gasoline engine. *J Combust Sci Technol*. 2022;28(1):1–10. https://doi.org/10.11715/rskxjs.R202011008.
50. Rashed A, Qasymeh M. Developing an interference-free non-destructive microwave testing system for liquid samples. In: *2018 IEEE 5th International Conference on Engineering Technologies and Applied Sciences 2018*. 2018:8629160. https://doi.org/10.1109/ICETAS.2018.8629160.
51. Rahaman MA, Hossain MK, Akhtar S, Shahadat HM. Dynamic viscosity and refractive index of aliphatic n-heptane with substituted aromatic hydrocarbons at T = (303.15 to 323.15) K and atmospheric pressure. *Chem Thermodynam Thermal Anal*. 2025;18:100188. https://doi.org/10.1016/j.ctta.2025.100188.
52. Bakshi A, Sharma C, Sharma AK, Sharma M. Probing the molecular interactions in some promising biofuel blends (prenol, 1-hexanol, 1-octanol, and 1-decanol): Volumetric, acoustic, and transport approach. *Chem Thermodynam Thermal Anal*. 2025;18:100185. https://doi.org/10.1016/j.ctta.2025.100185.
53. Handte T, Bohm S, Goj B, et al. Compact MEMS-based sensor for refractive index monitoring of liquids. *Sensor Actuator Phys*. 2025;386:116328. https://doi.org/10.1016/j.sna.2025.116328.
54. Howe A, Martino M, Richardson KA, Gaume R. Total uncertainty of a prism-coupling refractometry instrument modified for the infrared. *Opt Eng*. 2025;64(2):024108. https://doi.org/10.1117/1.OE.64.2.024108.
55. Krishna GN, Rahiman MK. A comparative study of pretreated Jatropha oil blended with ethanol and diesel for refractive index by novel Lorentz–Lorentz mixing method. *AIP Conf Proceed*. 2024;3193(1):020018. https://doi.org/10.1063/5.0232760.
56. Álvarez-Sanchis JA, Kovylina M, Vidal B. Terahertz refractometer based on extraordinary optical transmission for characterization of liquid samples. *IEEE Sens J*. 2024;24(9):14197–14204. https://doi.org/10.1109/JSEN.2024.3377271.
57. Shapiro TN, Lobakova ES, Dolnikova GA, et al. Community of hydrocarbon-oxidizing bacteria in petroleum products on the example of TS-1 aviation fuel and AI-95 gasoline. *Biotekhnologiya*. 2021;37(1):54–68. https://doi.org/10.21519/0234-2758-2021-37-1-54-68.
58. Resen DA, Altemimi MF. Advanced all-optical FBG refractometer for high-accuracy measurements. *J Opt*. 2024;53(1):728–733. https://doi.org/10.1007/s12596-023-01504-3.
59. Abbe E. Uber die Grenzen der geometrischen Optik/Mit Vorbemerkungen iiber die Abhandlung von Altmann. *S - Ber Jenaisch Ges Med Naturwiss*. 1890;346 p.
60. Abbe E. Messapparete fur physiker. In: *Gesammelte Abhandlungen Bd*. II. 1889:206–211.
61. Link F, De Klerk A. Viscosity and density of narrow distillation cuts from refined petroleum- and synthetic-derived distillates in the −60 to +60 °C range. *Energy Fuels*. 2022;36(20):12563–12579. https://doi.org/10.1021/acs.energyfuels.2c02625.
62. Das AK. Shedding light on insulation: probing the varied effects of illumination and storage temperatures on vegetable oil quality. *IEEE Trans Dielectr Electr Insul*. 2024;31(5):2803–2810. https://doi.org/10.1109/TDEI.2024.3400765.
63. El-Naggar AY, El-Adly RA, Altalhi TA, et al. Oxidation stability of lubricating base oils. *Petrol Sci Technol*. 2018;36(3):179–185. https://doi.org/10.1080/10916466.2017.1403450.